

Javier Fernández, Sourav Chatterjee, Volkan Degirmenci and Evgeny V. Rebrov*

Scale-up of an RF heated micro trickle bed reactor to a kg/day production scale

DOI 10.1515/gps-2015-0035

Received May 8, 2015; accepted July 20, 2015; previously published online September 1, 2015

Abstract: The scale-up of a radiofrequency (RF) heated micro trickle bed reactor for hydrogenation of 2-methyl-3-butyne-2-ol (MBY) over a Pd/TiO₂ catalyst has been performed. The axial and radial temperature profiles were calculated using a 2D convection and conduction heat transfer model. The effect of the reactor length, tube diameter and number of parallel tubes on the temperature non-uniformity parameter has been studied. The axial scale-up was achieved by repeating a single periodic unit consisting of one heating and one catalytic zone along the reactor length. The catalyst loading can be increased by an order of magnitude following this approach. A radial temperature difference of 2 K was developed in a reactor with an inner diameter of 15 mm. The scale-up by numbering up allows the accommodation of seven parallel tubes inside a single RF coil. It creates a 7 K difference in the average temperature between the central and the outer tubes which results in a 5% difference in MBY conversion. An overall scale-up factor of near 700 is achieved which corresponds to a production rate of 0.5 kg of product/day.

Keywords: fine chemicals; magnetic nanoparticles; micro reactor; radiofrequency; scale-up; trickle bed.

Nomenclature

a_s	external specific surface area of the catalyst (m ²)
B	magnetic field (T)
C_a	Carberry number

C_p	heat capacity (J/kg K)
C_F	Forchheimer drag coefficient
D	molecular diffusivity of MBY in methanol (m ² /s)
d_p	particle diameter (m)
E_a	activation energy (kJ/mol)
h_w	wall heat transfer coefficient (W/m ² K)
k_s	liquid-solid mass transfer coefficient
I	identity matrix
l	length of the induction coil (mm)
L	reactor length (mm)
P	pressure (Pa)
Pe	Peclet number
q_v'''	volumetric heat generation (kW/m ³)
R_{MBY}	reaction rate of MBY conversion (mol/kg s)
r_i	reaction rate of component i (mol/m ³ s)
Sh	Sherwood number
t	time (s)
T	temperature (K)
u	gas superficial velocity (m/s)
\vec{V}	superficial velocity (m/s)
z	spatial coordinate (m)

Greek letters

ΔH_{ads}	enthalpy variation for adsorption (kJ/mol)
ρ	density (kg/m ³)
ε_b	bed porosity (-)
k	thermal conductivity (W/m·K)
μ	viscosity (cP)
K_i	Equilibrium adsorption constant for component i
k_i	Kinetic constant for component i (mol/kg _{cat} s Pa)
λ_{eff}	Effective thermal conductivity
δ	Temperature non-uniformity parameter (%)

1 Introduction

The fine chemicals synthesis processes require the production of valuable compounds with a high degree of purity [1]. These processes, often multiphase in nature, commonly follow stoichiometric organic routes which generate substantial amounts of by-products and tend to suffer from low product yields [2]. Stringent environmental regulations based on good manufacturing processes make it necessary to replace existing stoichiometric processes with catalytic ones [3]. Batch processes are often chosen in fine chemicals synthesis because optimized

*Corresponding author: Evgeny V. Rebrov, School of Engineering, University of Warwick, Coventry CV4 7AL, UK; and School of Chemistry and Chemical Engineering, Queen's University Belfast, Belfast BT9 5AG, UK, e-mail: E.Rebrov@warwick.ac.uk.
http://orcid.org/0000-0001-6056-9520

Javier Fernández and Volkan Degirmenci: School of Engineering, University of Warwick, Coventry CV4 7AL, UK, http://orcid.org/0000-0003-2550-1875 (V. Degirmenci)

Sourav Chatterjee: School of Chemistry and Chemical Engineering, Queen's University Belfast, Belfast BT9 5AG, UK

reaction conditions can directly be transferred from a laboratory scale to a production scale. However, the stirred tank reactors have various drawbacks, such as labor intensive operation and poor performance as a result of insufficient mixing.

The chemical industry identifies process intensification and green catalytic engineering as the main strategy for future sustainable development [4, 5]. Improving industrial sustainability requires changing production at the process and system levels. In the near future, the classical large-scale chemical plants will be phased out [6] and novel microstructured plants will be coming to the market via the application of new customized process-flow modules. These micro reactor plants allow precise control of process parameters to obtain better yield and selectivity, which leads to easier, less energy intensive downstream separation.

Therefore, development of new and innovative reactor systems for catalytic chemical reactions has gained considerable attention recently [7, 8]. In particular, structured reactors are considered to offer numerous advantages in processing of moderate amounts of liquid reactants when compared with traditional stirred tank reactors. Improved mass and heat transfer properties enable the use of more intensive reaction conditions that result in higher reaction rates than those obtained with conventional reactors. Furthermore, heat management during exothermic reactions can properly be tuned.

Trickle bed reactors could be superior to stirred tank reactors, as there is no need for catalyst filtration [9]. Trickle bed reactors are employed in petrochemical and biochemical industries as well as in waste treatment applications [10]. However, poor heat transfer behavior of conventional trickle bed reactors and liquid flow maldistribution [11] often result in lower selectivities and catalyst deactivation [12]. The former is often caused by the fact that the heat is supplied from an external heating source and the net energy flux transferred to the reactor is a strong function of the wall heat transfer coefficient and thermal conductivity of the bed [13]. Several studies discuss the effect of these parameters on reactor performance [14, 15]. High thermal inertia of furnaces and low thermal conductivity of reactor beds makes it difficult to maintain isothermal conditions. The heat transfer to the center of a catalyst layer can still be a limiting step. Alternative means of energy supply that would facilitate rapid and uniform volumetric heating are therefore of interest.

Zonal radiofrequency (RF) heating of the structured support can enhance energy utilization. Zonal heating using microwaves was proved to be a scalable method which is demonstrated at laboratory scale [16]. In such

reactors, the reactor bed is packed with alternating zones of inert and absorbing particles, or the catalyst is deposited onto a structured support as a thin shell [17]. By the rational design of the bed packing, near isothermal conditions can be created inside the catalyst bed under microwave [16] or RF heating [8]. Moreover, combining continuous operation and RF heating as an alternative energy source, allows the accurate control of residence times in chemical processes. The synergism of RF heating and continuous operation leads to a process intensified approach, which improves the selectivity and product yield, thus increasing the output per unit volume of plant space [18, 19].

The scaling up of an RF heated reactor is to some extent similar to a microwave heated flow reactor. Most studies in this area evaluate the limitations related to the volumetric scale-up while using standard microwave equipment available in the market [20]. Comer and Organ [21], in their work on microwave assisted organic synthesis, discussed the possibility of parallelization of reactor tubes. While this work does not focus on scale-up, it addresses the possibility of synthesis of an organic library in multiple parallel tubes.

One of the suitable approaches for scaling up in continuous synthesis under RF heating is numbering up. The numbering up approach is based on the one hand, on numbering up of heating and catalytic zones in the axial direction inside a single tube [22] and on the other hand, on parallelization of tubular structured reactors with a channel diameter in the millimeter range [17], which can still be positioned inside a single RF coil. The former methodology has been employed in our previous study, where several heating and catalytic zones were placed inside a 70 mm long single tube reactor. Until recently, the later methodology presented itself as a challenge, as it requires an equal gas and liquid flow distribution among all parallel tubes. To solve this problem, Al-Rawashdeh et al. [23] developed a novel concept for a barrier based multiphase flow distributor. This distributor allows a uniform distribution of the gas and liquid flows over the microchannels when the pressure drop over the upstream barrier channels is about 5–20 times higher than the pressure drop over the corresponding reactor channels to be obtained. Gas-liquid channeling is prevented at equal pressures in the gas and liquid manifolds. The concept has been proven in a wide range of liquid flow rates and liquid to gas ratios [24]. With such an approach, a multitubular design of RF heated micro trickle bed reactor becomes feasible.

There exists also a possibility to increase the tube diameter upon scale-up. This is an additional advantage

of RF heating as compared to microwave heating, as the penetration depth of RF waves is in the meter range. Therefore, the magnetic field remains rather uniform over the reactor cross section and it depends mainly on the coil geometry rather than on magnetic properties of the absorbing material; it is therefore temperature independent. However, this scale-up approach still should be based on the modelling as characteristic time for conduction changes as the reactor diameter increases.

Catalytic hydrogenation is an important type of gas-liquid-solid reaction in pharmaceutical and fine chemical industries [4]. The catalytic hydrogenation of acetylene alcohols is an important reaction used in the synthesis of vitamins A and E [25], as well as fragrances such as linalyl acetate, linalool, and dimethyloctenol [26]. The state-of-the-art industrial technology for catalytic hydrogenation is based on stirred tank reactors over Pb-doped Pd catalysts [26]. Recent developments suggest that titania supported noble metal catalysts can be employed for this reaction [25, 27]. The catalytic hydrogenation of D-glucose to D-sorbitol is of great industrial importance, as the latter is widely used as an additive in foods, drugs, and cosmetics [28]. D-glucose is currently produced commercially via the enzymatic hydrolysis of starch. The direct production of D-glucose from nonedible biomass [29, 30] renders opportunities for the efficient utilization of biomass feedstocks through D-glucose hydrogenation to sugar alcohols [28], conversion to furan type platform compounds [31–33] and organic acids [34], and their further catalytic hydrogenation [35].

This work reports the scale-up of an RF heated micro trickle bed reactor by using a multitubular approach. This is achieved, among others, by providing a uniform temperature distribution in all parallel tubes of the reactor assembly. The performance of the multitubular assembly in hydrogenation of 2-methyl-3-butyne-2-ol (MBY) was evaluated and compared with a single tube reactor. The temperature profiles were obtained by a 2D convection and conduction model with a heat generation term accounting for the actual distribution of magnetic field inside the catalyst bed. The obtained temperature profiles were validated experimentally for a selected number of experiments.

2 Modelling

The steady-state temperature profiles in the reactor (length 210 mm, diameter 5–50 mm) were obtained by a 2D convection and conduction model [8, 22] which

was solved numerically in COMSOL Multiphysics 5.0. Around 100,000 mesh elements were used to reach mesh independent solutions in all calculations. Heat transfer phenomena in the RF heated reactor are described by the conservation equations of mass, momentum, and energy leading to a set of nonlinear partial differential equations. To simplify the analysis, the fluid flow is assumed to be non-compressible and the catalyst particles are assumed to be spherical with a diameter d_p . Moreover, the catalyst bed is treated as a homogeneous porous medium with porosity ε_b and permeability K . Based on the above assumptions, the governing equations for the mass conservation and fluid flow can be written as:

$$\nabla \cdot (\varepsilon_b \rho \vec{V}) = 0 \quad (1)$$

$$\frac{1}{\varepsilon_b^2} \nabla \cdot (\rho \vec{V} \vec{V}) = \nabla \cdot \left[-p \vec{I} + \frac{\mu}{\varepsilon_b} (\nabla \vec{V} + (\nabla \vec{V})^T) - \frac{2\mu}{3} \vec{I} \nabla \cdot \vec{V} \right] + S_u \quad (2)$$

where \vec{V} is the superficial velocity, μ is the viscosity, and p is pressure. The source term, S_u , term:

$$S_u = -\frac{\mu}{K} \vec{V} + \frac{\rho C_F}{\sqrt{K}} |\vec{V}| \vec{V} \quad (3)$$

K is the permeability and C_F is the Forchheimer drag coefficient for a packed bed of spherical particles with homogenous porosity can be, respectively, given as:

$$K = \frac{d_p^2 \varepsilon_b^3}{150(1-\varepsilon_b)^2} \quad (4)$$

$$C_F = \frac{1.75}{\sqrt{150} \varepsilon_b^{1.5}} \quad (5)$$

The heat transfer in porous media is described by Eq. (6):

$$\nabla \cdot (\varepsilon_b \rho C_p \vec{V} T) = \nabla \cdot (\lambda_{eff} \nabla T) + q_V''' + h_w a (T - T_\infty) \quad (6)$$

where a is the external wall area per unit of the reactor volume, λ_{eff} is the effective thermal conductivity of the catalyst bed, h_w is the wall heat transfer coefficient, T is the temperature, ρ is the fluid density, q_V''' is the volumetric heat generation, and C_p is the fluid specific heat capacity. q_V''' is proportional to the magnetic field which is adapted from Mispelter [36]:

$$q_V''' = q_0 \left[\frac{z+l/2-L/2}{\sqrt{r^2 + (z+l/2-L/2)^2}} - \frac{z-l/2-L/2}{\sqrt{r^2 + (z-l/2-L/2)^2}} \right] \quad (7)$$

where q_0 is the maximum volumetric heat generation at the center of the coil, l is the length of the coil, and L is the length of the reactor. q_V''' is zero in the catalytic zones.

The no-slip boundary condition was used at the reactor walls. The actual inlet liquid velocity and an outlet pressure of 1 bar were chosen as boundary conditions for the fluid flow model. For the heat transfer case, heat flux at the reactor walls and an inlet temperature of 293 K were chosen as boundary conditions. The fluid properties of methanol were used in simulations.

The catalyst bed was segmented into several sections positioned between adjacent heating zones. The kinetic model for hydrogenation of MBY was adopted from [25] to calculate the conversion. The kinetic parameters are listed in Table 1 and the reaction mechanism is given in Scheme 1. The reaction is zero order in MBY and first order in hydrogen [25]. Therefore, in general, the reaction rate depends on the hydrogen partial pressure. However, as the pressure drop in the reactor is 1 kPa which is 0.1% from the absolute pressure and the hydrogen consumption does not exceed 0.5% even at a full MBY conversion, it can safely be assumed that the reaction rate depends only on the catalyst temperature.

Simulations were performed to determine the minimum number and the length of each heating zone which would provide an isothermal profile in the fixed bed. The reactor parameters were adapted from [8] and they are listed in Table 2. A higher volumetric heat generation rate of 0.3 W/cm³ was fixed in the preheating section to reduce its length. In an actual reactor, this is done by providing a higher ferrite loading in the preheating zone.

Table 1: Kinetic parameters for 2-methyl-3-butyne-2-ol (MBY) hydrogenation.

Parameter	Unit	Value
k_{10}	s ⁻¹	5×10 ⁸
k_{20}	s ⁻¹	6×10 ⁷
k_3	s ⁻¹	2.4×10 ⁻⁴
E_{MBA}	J/mol	60,300
E_{MBE}	J/mol	42,000
K_Y	m ³ /mol	20
K_E	m ³ /mol	3.5×10 ⁻²
K_A	m ³ /mol	1.3×10 ⁻²



Scheme 1: Reaction pathways of 2-methyl-3-butyne-2-ol (MBY) hydrogenation into products of 2-methyl-3-buten-2-ol (MBE) and 2-methyl-3-butan-2-ol (MBA).

Table 2: Thermophysical reactor parameters.

Parameter	Unit	Value
Heat transfer coefficient	W/(m ² ·K)	4.5
Effective thermal conductivity of bed	W/(m·K)	4.0
Ferrite density	kg/m ³	5000
Ferrite specific heat capacity	J/(kg·K)	700
Catalyst density	kg/m ³	2460
Catalyst specific heat capacity	J/(kg·K)	770
Bed porosity	–	0.43

3 Materials and methods

3.1 Materials

All chemicals were purchased from Sigma Aldrich, UK. The hydrogenation of MBY was performed over a 1.2 wt% Pd/TiO₂ catalyst prepared by incipient wetness impregnation of P25 titania (Degussa) with a palladium chloride solution (Sigma Aldrich). The catalyst was calcined at 673 K for 4 h. Prior to reaction, the catalyst was reduced *in situ* with hydrogen at 473 K. The nickel ferrite pellets (106–150 μm) were used as heating material. They were prepared following the procedure reported in Ref. [37].

3.2 Reactor

A vertically positioned tubular quartz reactor (inner diameter 10 mm, outer diameter 12.7 mm) was filled with several zones of nickel ferrite particles [37] separated by catalytic zones according to the approach described in our previous work [8, 22] (Figure 1). The structured bed was fixed from both sides with two porous PEEK plates. The reactor was placed inside an 11-turn induction coil with an inner diameter of 26 mm and a length of 210 mm. The induction coil was connected to an RF generator operating at 180 kHz (Easyheat Ambrell). The reactor and the coil were insulated with glass wool of 4 cm thickness.

A fiber optic temperature sensor (accuracy of 0.1 K, FISO Scientific) was placed inside a glass capillary (outer diameter 3.0 mm) along the central axis of the bed for temperature measurements. The temperature at a specific position was controlled with the LABVIEW software. A solution of MBY (0.3 mol/l in methanol) was fed in the reactor with an HPLC pump (Shimadzu LC-20AT). The liquid flow rate was varied between 0.2 ml/min and 0.3 ml/min. The co-current 66 vol% H₂ in He flow (total flow rate: 3.0 ml/min) was fed with a mass flow controller (Brooks). The gas and liquid flows were mixed in a T-mixer prior to the reactor. The liquid was separated from the gas at the reactor exit with a gas-liquid microseparator. MBY and the reaction products were analyzed by Shimadzu GC-2010 gas chromatograph using a CP-sil 5CB capillary column (length 30 m, internal diameter 250 μm, film thickness 1.0 μm, Agilent) and using a flame ionization detector.

The liquid hold-up in the reactor is 0.89±0.01 and it does not depend on the gas flow rate. Therefore, the obtained flow regime is

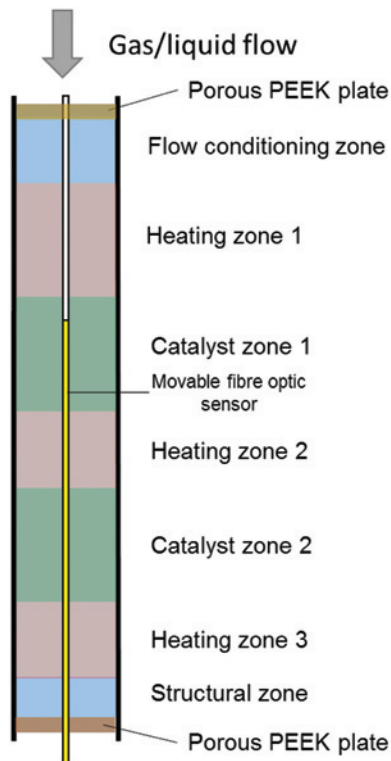


Figure 1: The schematic representation of the reactor showing heating and catalytic zones.

similar to that observed in a single phase (liquid only) reactor [8]. The absence of mass transfer limitations was verified in our previous study [22] where it was demonstrated that the reaction rate does not depend on the liquid flow rate and the apparent activation energy is close to that earlier reported over the Pd/TiO₂ catalyst [25]. Theoretically, the absence of liquid-solid mass transfer limitations is confirmed from the Carberry number of 0.002 [Eq. (8)] which is far below the critical value of 0.05:

$$Ca_{MBY} = \frac{R_{MBY}}{k_{s,MBY} \cdot a_s \cdot C_{MBY}} \quad (8)$$

where R_{MBY} is the measured reaction rate of MBY of $1.7 \cdot 10^{-4}$ mol/(kg·s), a_s is the external specific surface area of the catalyst, and k_s is the liquid-solid mass transfer coefficient. The external surface area of the catalyst is estimated to be 20 m²/kg, from a mean spherical particle diameter of 128 μm and a P25 porosity of 40%. The maximum reactant concentration (C_{MBY}) is 300 mol/m³. The liquid-solid mass transfer coefficient was calculated by Eq. (9):

$$k_s = \frac{Sh \cdot D}{d_p} = 1.3 \cdot 10^{-5} \quad (9)$$

where D is the molecular diffusivity of MBY in methanol ($D = 0.6 \cdot 10^{-9}$ m²/s) and Sherwood number (Sh) number was estimated from a single phase flow correlation for packed bed at low Peclet (Pe) numbers [38]:

$$Sh = 1.09 \varepsilon^{-1} Pe^{0.33} = 2.7 \quad (10)$$

4 Results and discussion

4.1 Scale-up in the axial dimension

It has been noticed [22] that in order to keep a low temperature non-uniformity, it is necessary to split a single catalytic zone into several sections separated by heating zones. One catalytic and one heating zone form a single periodic unit which, in principle, can be repeated in the axial direction if the RF field uniformity remains the same. That assumption would be valid if (i) the heat released by an exothermic hydrogenation reaction is at least an order of magnitude below that produced by the magnetic particles in heating zones and (ii) the heat loss by natural convection via the external wall remains the same over the entire length of the reactor. In that case, the net heat generation rate over a single periodic unit is equal to the rate of heat loss to the environment, the latter being determined by natural convection.

The first assumption can be satisfied at a relatively high concentration of magnetic particles in the heating zones. In this case, any change of reaction rate would not influence the overall heat production rate. The second assumption is valid for a relatively short reactor ($L/d < 100$) when the development of natural convection boundary layer occurs in the laminar regime.

The temperature profile in the single tube reactor was obtained by solution of a 2D convection and conduction model [Eq (1)–Eq. (5)]. In this design, 10 catalyst bed sections with a length of 10 mm were separated by 11 heating zones with a length of 5 mm. The first heating zone was required to preheat the reaction mixture from room temperature to the reaction temperature.

It can be seen that the temperature rises from 290 K to the reactor set-point (314 K) within the first 35 mm of the reactor length and then remains rather constant (Figure 2A). Local temperature maxima develop within the heating zones, while local minima are observed in the catalytic zones. The periodic repetition of one catalytic and one heating zone allows keeping the temperature non-uniformity within 2 K. The MBY conversion increases linearly with the residence time in the catalytic zones following a zero order kinetics until a conversion of 99% is reached in catalytic zone 6 (Figure 2B). The subsequent catalytic layers (from zone 7 to 11) can be added in case of catalyst deactivation or when a higher liquid flow rate would be required. Otherwise, they can be omitted and replaced by inert material. As the total pressure drop does not exceed 1.0 kPa, it is rather straightforward to build up a reactor bed of any length by repeating the single periodic unit.

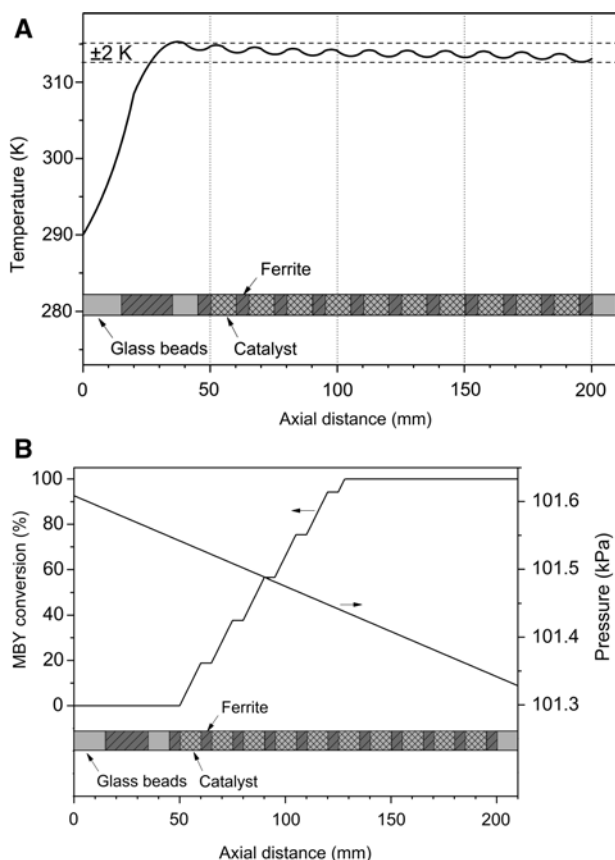


Figure 2: Simulated (A) temperature, (B) 2-methyl-3-butyne-2-ol (MBY) conversion and pressure drop as a function of axial position in the 11 zone micro trickle bed reactor. Liquid flow rate: 0.1 ml/min gas flow rate: 3.0 ml/min (STP) volumetric heat generation rate: 410 kW/m³.

4.2 Scale-up in the radial dimension

The scale-up in the axial direction can potentially increase the productivity of a single zone reactor by an order of magnitude. Still there is a possibility to extend the catalyst volume in the radial dimension while maintaining near-isothermal operation of the reactor bed. In order to investigate the effect of reactor diameter on the temperature non-uniformity parameter and conversion, temperature distribution was investigated in reactors with diameters of 5 mm, 10 mm, 15 mm, 25 mm and 50 mm. Those will be designated as R-a, where a is the diameter in mm, hereafter.

As opposed to the axial scale-up, the intensity of the magnetic field changes in the radial direction, therefore the heat generation term cannot be considered as constant over the cross section of the reactor. Therefore, the heat generation term was introduced as a function of radial

position. The total amount of heat was adjusted to keep the same average temperature in the reactor. This is due to the fact that volumetric heat generation rate increases faster ($\sim r^3$) than the external surface area ($\sim r^2$) as the diameter increases. Therefore the amount of magnetic material in the heating zones was reduced as the reactor diameter increases.

The temperature distribution in the R-5, R-15 and R-50 reactors is shown in Figure 3A. It can be seen that there is no radial temperature gradient in the R-5, a small radial temperature gradient starts to develop in the downstream section of R-15, and a substantial gradient develops in R-50 as the temperature decreases towards the outer surface.

The temperature non-uniformity results in different reaction rates over the reactor cross section and this results in different conversion levels in these three reactors as shown in Figure 3B. A temperature difference of 2 K between the wall temperature and center axis temperature is created at a diameter of 15 mm (Figure 4). Therefore, this diameter is chosen for the subsequent numbering up study. This reactor can accommodate a 9-fold amount of catalyst which results in a comparable enhancement in productivity to that in the axial scale-up.

4.3 Scale-up by numbering up

Increasing the reactor dimensions has a beneficial effect as the production rate increases by two orders of magnitude. Still there exists a possibility to increase the production rate via a numbering up approach. Due to their lower frequency levels, RF waves have a larger penetration depth than microwaves and hence could find better application in larger size reactors. As the penetration depth of the RF field is much higher as compared to the tube diameter (15 mm), the intensity of magnetic field remains relatively constant over the cross section of a single tube. This is impossible for most liquids heated by microwaves.

However, there is a distribution of a magnetic field in the radial dimension of a coil. Upscaling of current RF systems, to provide a uniform magnetic field pattern in commercial-scale processes, still remains a major challenge. This results in different steady state conversions in a central and outer tubes in a multitubular reactor which consists of seven parallel tubes: one central and six outer tubes.

Being in the highest field intensity region, the central tube gave the highest conversion (Figure 5A). The outer

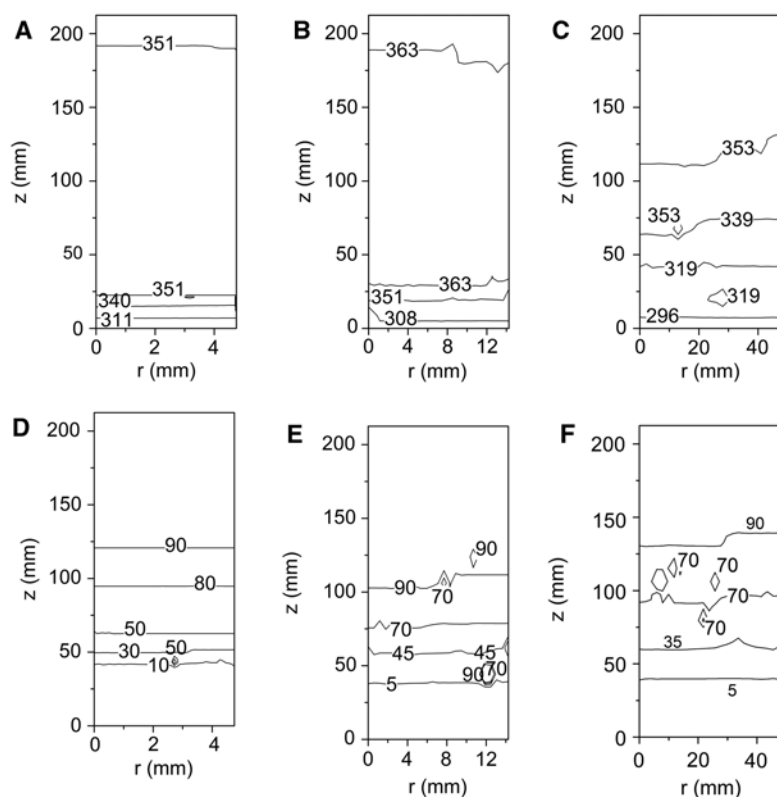


Figure 3: Temperature (A–C) and 2-methyl-3-butyn-2-ol (MBY) conversion (D–F) maps in the 11 zone reactors. Reactors: (A, D) R-5 mm, (B, E) R-15, (C, F) R-50 mm. Reaction conditions are the same as those in Figure 2.

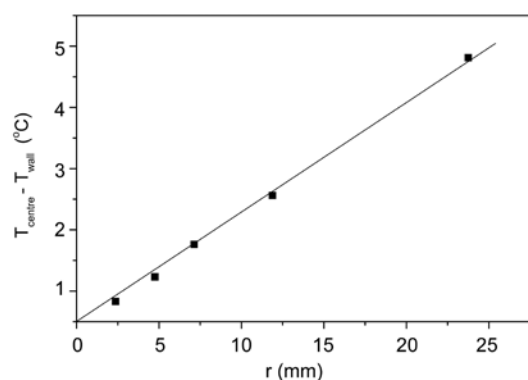


Figure 4: The temperature non-uniformity as a function of reactor radius. Reaction conditions are the same as those in Figure 2.

tubes being exposed to a weaker magnetic field as compared to the central tube gave a lower conversion. This is due to the difference in local temperature distribution both in axial (Figure 5B) and radial directions (Figure 5C and D). The average temperature in the central tube is 366 K, whereas it is 359 K in the outer tubes. This results in a 5% difference in the overall MBY conversion. Such a

difference can be considered as acceptable for most industrial applications. However, if a higher degree of product uniformity is required, it is better to keep the central reactor position empty.

5 Experimental validation

The reactor design was verified experimentally in the hydrogenation of MBY. The reactor was loaded with three, four or five catalytic zones containing the 1.2 wt% Pd/TiO₂ catalyst (50 mg per zone) while the remaining catalytic zones were filled with an inert material which has the same thermal properties as the actual catalyst. The initial concentration of MBY was fixed at 0.7 mol/l and the liquid flow rate was fixed at 0.1 ml/min. A good agreement between experimental and modelling results was observed. It can be seen that temperature at the axial positions from $x=35$ to 200 mm remains within 2 K from the reactor set-point of 313 K (Figure 6A). The MBY conversion and MBE selectivity also demonstrated a good agreement with the model predictions. Figure 5B shows a comparison between experimental and modelling results for a configuration with five catalytic

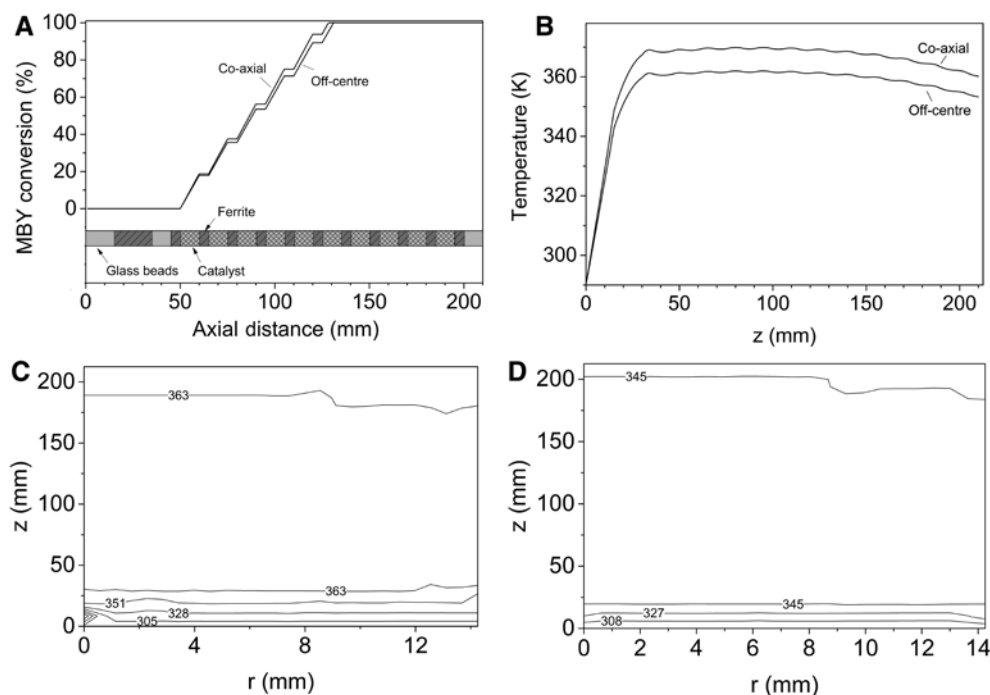


Figure 5: (A) 2-Methyl-3-butyn-2-ol (MBY) conversion and (B) center axis temperature in the 11 zone R-15 reactors as a function of axial position, (C, D) temperature maps of R-15 reactor positioned (C) in the center of the coil (D) near the edge (see Figure 7). Reaction conditions are the same as those in Figure 2.

layers. It can be seen that an MBY conversion of 94% and MBE selectivity of 70% were obtained in this experiment, which is in excellent agreement with predictions made by the reactor model. A pressure drop of 1 kPa was observed in this reactor configuration, which is in line with the theoretical prediction (Figure 2B). The conversion remained stable for several days of operation without substantial increase in the pressure drop. This could justify the feasibility of the chosen scale-up approach. Furthermore, it can be concluded that the 2D convection and conduction model could adequately predict the reactor behavior.

6 Scale-up methodology

The scale-up method is divided into three steps – a repetition of a single periodic unit composed of one catalytic and one heating zone (Figure 7A) along the reactor length (Figure 7B), an increase of reactor diameter (Figure 7C) and a numbering up step (Figure 7D).

The repetition of the single periodic unit results in a scale-up factor of at least 11, which is proven in this study. There is still a possibility of increasing the number of periodic units in the axial direction as the pressure drop

over the reactor bed remains relatively low and it does not result in densification of the reactor bed.

The scale-up in the radial direction depends on the thermophysical properties of the catalytic bed. In general, trickle bed reactors suffer from low effective thermal conductivity, which does not allow increase in the reactor diameter without substantial increase in the radial temperature gradient. In this study, the titania support was used for the Pd catalyst, which has relatively low thermal conductivity. This still allows an increase in the reactor diameter by 3 times as compared to a laboratory scale reactor, which results in a 9-fold increase of productivity. A combination of axial and radial scale-up could provide an increase of two orders of magnitude in production rate (Table 3).

Finally, scale-up by numbering up allows accommodation of up to seven parallel tubes inside a typical RF coil. There is a substantial difference between the central and outer tubes, which is due to different intensity of magnetic fields at these positions. This non-uniformity can further be adjusted by placing different amounts of ferrite material in the central and outer tubes. A higher loading of magnetic material in the heating zones would compensate for lower intensity of magnetic field in the peripheral tubes.

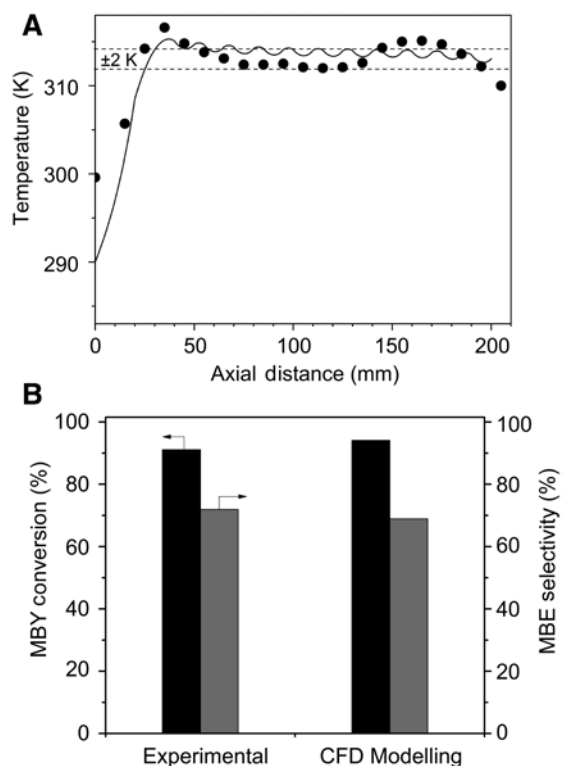


Figure 6: (A) Measured (symbols) and predicted (line) temperature along the center axis in the 11 zone R-5 reactor. (B) Measured and predicted 2-methyl-3-butene-2-ol (MBY) conversion and 2-methyl-3-butene-2-ol (MBE) selectivity in the 5 catalytic zone R-5 reactor. Reaction conditions are the same as those in Figure 2.

Table 3: Scale-up factors for different methods.

	A	R	N	A+R	A+N	A+R+N
Scale-up factor	11	9	7	99	77	693

A, axial; N, numbering up; R, radial.

In total, a scale-up factor of almost 700 ($11 \times 9 \times 7$) can be achieved in this approach. This translates in an overall production rate of 0.5 kg of product/day. This design requires an efficient gas liquid distributor to uniformly feed a system of parallel tubes.

7 Conclusions

A scale-up method was proposed for a micro trickle bed reactor. The method is divided into three steps – a repetition of a single periodic unit composed of one catalytic and one heating zone along the reactor length, an increase of reactor diameter and a numbering up step. This scale-up approach is based on maintaining the temperature non-uniformity parameter in the reactor at the constant level. It requires only lab scale data and it reduces significantly the risk of failure during the initial scale-up of the process.

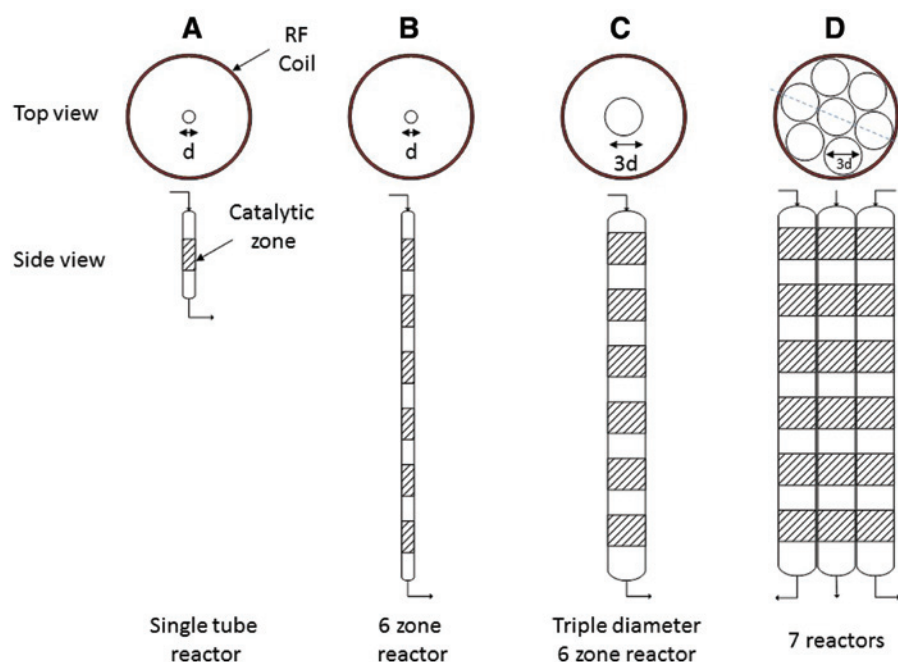


Figure 7: Schematic representation of the scale-up methodology. (A) Laboratory scale micro trickle bed reactor, (B) axial scale-up, (C) radial scale-up, (D) scale-up by numbering up.

The optimum reactor configuration was simulated using a convection and conduction heat transfer model and the numerical results were in very good agreement with experimental data. The overall productivity in a hydrogenation reaction was increased by a factor of 700 using this approach.

Acknowledgments: The financial support provided by the European Research Council (ERC), project 279867, is gratefully acknowledged.

References

- [1] Mohamed HM. *TrAC. Trends Anal. Chem.* 2015, 66, 176–192.
- [2] Pfaltzgraff LA, Clark JH. In *Advances in Biorefineries*, Waldron K, Ed., Woodhead Publishing: Amsterdam, 2014, pp 3–33.
- [3] Mills PL, Chaudhari RV. *Catal. Today* 1997, 37, 367–404.
- [4] Philippe M, Didillon B, Gilbert L. *Green Chem.* 2012, 14, 952–956.
- [5] Hessel V, Kralisch D, Krtschil U. *Energy Environ. Sci.* 2008, 1, 467–478.
- [6] Belloni A. *Process* 2006, 13, 64–65.
- [7] De Wilde J, Froment GF. *Fuel* 2012, 100, 48–56.
- [8] Chatterjee S, Degirmenci V, Aiouache F, Rebrov EV. *Chem. Eng. J.* 2014, 243, 225–233.
- [9] Stitt EH. *Chem. Eng. J.* 2002, 90, 47–60.
- [10] Al-Dahhan MH, Larachi F, Dudukovic MP, Laurent A. *Ind. Eng. Chem. Res.* 1997, 36, 3292–3314.
- [11] Boelhouwer JG, Piepers HW, Drinkenburg AAH. *Chem. Eng. Sci.* 2001, 56, 1181–1187.
- [12] Hessel V, Angeli P, Gavriilidis A, Loewe H. *Ind. Eng. Chem. Res.* 2005, 44, 9750–9769.
- [13] Babu V, Sastry KKN. *Comput. Chem. Eng.* 1999, 23, 327–339.
- [14] Lamine AS, Gerth L, Le Gall H, Wild G. *Chem. Eng. Sci.* 1996, 51, 3813–3827.
- [15] Houlding TK, Rebrov EV. *Green Process Synth.* 2012, 1, 19–31.
- [16] Benaskar F, Patil NG, Rebrov EV, Ben-Abdelmoumen A, Meuldijk J, Hulshof LA, Hessel V, Schouten JC. *Chem. Sus. Chem.* 2013, 6, 353–366.
- [17] Patil NG, Benaskar F, Rebrov EV, Meuldijk J, Hulshof LA, Hessel V, Schouten JC. *Ind. Eng. Chem. Res.* 2012, 51, 14344–14354.
- [18] Houlding TK, Tchabanenko K, Rahman MT, Rebrov EV. *Org. Biomol. Chem.* 2013, 11, 4171–4177.
- [19] Houlding TK, Gao P, Degirmenci V, Tchabanenko K, Rebrov EV. *Mater. Sci. Eng. B* 2015, 193, 175–180.
- [20] Matsuzawa M, Togashi S, Hasebe S. *J. Therm. Sci. Tech.* 2011, 6, 69–79.
- [21] Comer E, Organ MG. *Chem. Eur. J.* 2005, 11, 7223–7227.
- [22] Chatterjee S, Degirmenci V, Rebrov EV. *Chem. Eng. J.* 2015, 281, 884–891.
- [23] Al-Rawashdeh M, Fluitsma LJM, Nijhuis TA, Rebrov EV, Hessel V, Schouten JC. *Chem. Eng. J.* 2012, 181–182, 549–556.
- [24] Al-Rawashdeh M, Yu F, Nijhuis TA, Rebrov EV, Hessel V, Schouten JC. *Chem. Eng. J.* 2012, 207–208, 645–655.
- [25] Rebrov EV, Klinger EA, Berenguer-Murcia A, Sulman EM, Schouten JC. *Org. Process Res. Dev.* 2009, 13, 991–998.
- [26] Bonrath W, Medlock J, Schütz J, Wüstenberg B, Netscher T. In *Hydrogenation*, Karame I, Ed., Intech: Rijeka, Croatia, 2012, pp 69–90.
- [27] Cherkasov N, Ibhaddon AO, Rebrov EV. *Lab Chip* 2015, 15, 1952–1960.
- [28] Mishra DK, Lee J-M, Chang J-S, Hwang J-S. *Catal. Today* 2012, 185, 104–108.
- [29] Van de Vyver S, Geboers J, Jacobs PA, Sels BF. *Chem. Cat. Chem.* 2011, 3, 82–94.
- [30] Degirmenci V, Uner D, Cinlar B, Shanks BH, Yilmaz A, van Santen RA, Hensen EJM. *Catal. Lett.* 2011, 141, 33–42.
- [31] Degirmenci V, Pidko EA, Magusin PCMM, Hensen EJM. *Chemcatchem* 2011, 3, 969–972.
- [32] Degirmenci V, Hensen EJM. *Environ. Prog. Sust. Energ* 2014, 33, 657–662.
- [33] Zhang Y, Degirmenci V, Li C, Hensen EJM. *Chemsuschem* 2011, 4, 59–64.
- [34] Luterbacher JS, Martin Alonso D, Dumesic JA. *Green Chem.* 2014, 16, 4816–4838.
- [35] Alonso DM, Wettstein SG, Dumesic JA. *Green Chem.* 2013, 15, 584–595.
- [36] Mispelner J. In *NMP Probeheads for Biophysical and Biomedical Experiments*, Imperial College Press: London, 2006.
- [37] Gao P, Hua X, Degirmenci V, Rooney D, Khraisheh M, Pollard R, Bowman RM, Rebrov EV. *J. Magn. Magn. Mater.* 2013, 348, 44–50.
- [38] Wilson EJ, Geankoplis CJ. *Ind. Eng. Chem. Fundam.* 1966, 5, 9–14.

Bionotes



Javier Fernández

Javier Fernández obtained his Bachelor's degree in Chemical Engineering in 2007 and his Master's degree in Environmental and Processes Engineering in 2010 from the University of Oviedo, Spain, while he worked in research activities for different companies such as Saint-Gobain and XSTRATA. In 2011, he started his PhD in Chemical Engineering working in the LOWCARB European Project. He received the *cum laude* Award in 2014 and then moved to the School of Engineering at the University of Warwick, where he is currently working as a postdoctoral researcher.

**Sourav Chatterjee**

Sourav Chatterjee obtained his BTech in Chemical Engineering from West Bengal University of Technology, India in 2010. He received his MSc (distinction) in Process Engineering in 2011 from Queen's University of Belfast, UK, having worked in the group of Professor Evgeny Rebrov. He continued his doctoral research in the same group and obtained his PhD in Chemical Engineering in 2014. He is currently working as a postdoctoral research fellow at Max Planck Institute of Colloid and Interfaces in Berlin, Germany.

**Volkan Degirmenci**

Volkan Degirmenci obtained his PhD in Chemical Engineering from Middle East Technical University, Ankara, Turkey, in 2007. He joined the School of Engineering at University of Warwick in 2015 as Assistant Professor. The research interests of Dr. Degirmenci are microporous and mesoporous materials, development of sustainable processes for biomass conversion, *in situ* spectroscopy for the understanding of the reaction mechanisms and structure-activity relations in heterogeneous catalysis, carbon dioxide capture and utilization and energy intensified reactor design.

**Evgeny V. Rebrov**

Evgeny V. Rebrov is full professor of Chemical Engineering in the School of Engineering at the University of Warwick since 2014. He got his PhD in Chemistry from the Boreskov Institute of Catalysis (Novosibirsk, Russia) in 1999. In 2011, the European Research Council awarded Professor Evgeny Rebrov a prestigious ERC Starting Grant to pursue frontier research in nontraditional energy sources. This ERC grant addresses the development of advanced composite magnetic microparticles to be applied for efficient and fast heating using RF field.